Synchronization in a Pair of Thermally Coupled Rotating Baroclinic Annuli: Understanding Atmospheric Teleconnections in the Laboratory

A. A. Castrejón-Pita and P. L. Read

Atmospheric, Oceanic & Planetary Physics, Clarendon Laboratory, University of Oxford, Parks Road, Oxford, OX1 3PU, United Kingdom

(Received 20 January 2010; revised manuscript received 29 March 2010; published 18 May 2010)

Synchronization phenomena in a fluid dynamical analogue of atmospheric circulation is studied experimentally by investigating the dynamics of a pair of thermally coupled, rotating baroclinic annulus systems. The coupling between the systems is in the well-known master-slave configuration in both periodic and chaotic regimes. Synchronization tools such as phase dynamics analysis are used to study the dynamics of the coupled system and demonstrate phase synchronization and imperfect phase synchronization, depending upon the coupling strength and parameter mismatch.

DOI: 10.1103/PhysRevLett.104.204501 PACS numbers: 47.52.+j, 05.45.Xt, 47.32.Ef, 92.60.Ry

Introduction.—The origin of oscillations and cyclic behavior in the weather and circulation of the atmosphere and oceans has long been of interest to scientists. Commonly cited examples include the El Niño/southern oscillation (ENSO), the North Atlantic oscillation (NAO)/arctic oscillation, the quasibiennal oscillation, and the zonal index cycle [1–4]. It has been suggested that certain fluctuations in meteorological records are characterized by ''teleconnection'' patterns, in the sense of significant correlations between the fluctuations of a field at widely separated points. Such correlations suggest that some kind of information is propagated between two (or more) distant places, through the atmosphere. For instance, teleconnections between chaotic middle latitude blocking of the northern and southern hemispheres have been diagnosed by [5]. Similar results have also been found in numerical general circulation models or coupled-hemisphere models [6–8]. In other teleconnection phenomena, attention has been directed towards regional events, such as in historic records of precipitation or the high water levels of major rivers such as the Nile. Such responses may be correlated with different cycles of climatic variables which could reflect a degree of nonlinear synchronization underlying such correlations (see [9–11]).

The study of synchronization in simple and controlled experimental analogs of atmospheric circulations may therefore be expected to provide a helpful and powerful source of insight in the study of climate variability. Detailed studies of synchronization in controlled laboratory experiments, especially in relation to continuum fluid systems, are still comparatively unusual, however, in part because of intrinsic difficulties in measurement and experimental control. In the present study, investigations of synchronization phenomena are presented in the context of two idealized analogues of midlatitude atmospheric circulation, namely, the thermally driven, rotating annulus experiment [12,13]. The experiment is traditionally interpreted as being analogous to a midlatitude baroclinic ''storm zone'' in either the northern or southern hemisphere of an Earth-like planet. The experiment studies the motion of a fluid in cylindrical-annular container, differentially heated in the horizontal (ΔT) and rotating (at angular velocity Ω) around the vertical axis of symmetry, emulating the temperature contrast between polar and tropical regions on Earth. Depending on the imposed parameters, the rotating baroclinic annulus system can exhibit a rich variety of dynamical phenomena and sequences of bifurcations, including highly coherent and symmetric patterns of periodic or quasiperiodic (modulated in amplitude) waves, transitions to low-dimensional chaotic states, and forms of geostrophic turbulence. In this work, we studied the effects of coupling two annuli exhibiting baroclinic waves, whose amplitude varied in time in either a quasiperiodic or chaotic regime.

Experimental setup.—The experiment consists of two annular containers, mounted one above the other on a turntable base so they can be rotated about their common vertical axis of symmetry. Each annulus comprises two concentric brass cylinders; the lid and the base are made of Perspex and Tufnol. The inner cylinders have a radius of $R_{\mathrm{inn}} = 25$ mm, while the outer cylinders have a radius of $R_{\mathrm{out}} = 80$ mm. The depth of each annulus is $h = 140$ mm. Inside the annular space, at mid-depth and midradius, a copper-constantan thermocouple ring is situated in each system, providing 32 measurement points, equally spaced in the azimuthal direction. Both annuli are arranged inside a temperature controlled enclosure in order to maintain a stable thermal environment to within $\pm 0.05\,^{\circ}\mathrm{C}$. The inner cylinders are cooled ($T = T^{\mathrm{inn}}$) and the outer ones are warmed ($T = T^{\mathrm{out}}$) by circulating water flows in spiral grooves inside the inner cylinders and outside the outer cylinders whose temperature is finely maintained via inline computer-controlled heaters. Experimental investigations carried out by [14] have shown that when amplitude vacillating (AV) flows are present in the annulus, the total heat transfer between the outer and inner walls is modulated in the same form as the vacillation of the flow, implying an oscillation in the temperature of the cooling water. The

coupling between the two annuli was achieved by connecting the output of the circulating coolant from the outer cylinder of the master annulus to the coolant input of the outer circuit of the slave annulus. By this means, dynamically induced variations in the horizontal heat transport within one experimental system led to fluctuations in the temperature of coolant fed to the second system in such a way that the dynamics of the first system could affect in real time the boundary conditions presented to the second system, while both systems were maintained on average at similar (though not identical) points in parameter space. Remotely controlled electric solenoid valves allowed the coupling to be turned on or off. A schematic diagram of the system is shown in Fig. 1

Experimental procedure.—The working fluid was a 25% (by volume) solution of glycerol in water, having a mean density of 1081 kg m^{-3} and a Prandtl number of 26.4. This system has been extensively studied by [14] in an essentially identical apparatus so that a comprehensive regime diagram was already available.

$\Delta T_S = T_S^{\text{out}} - T_S^{\text{inn}}$ was maintained at $\simeq 10.0\,^\circ$C for the slave system and was varied from $\Delta T_M = T_M^{\text{out}} - T_M^{\text{inn}} \approx 9.5$–$10.5\,^\circ$C for the master; two rotation rates were used, $\Omega_P = 1.736$ rad/s and $\Omega_C = 1.621$ rad/s, for the periodic and chaotic cases, respectively (the combination of the chosen Ω_C and $\Delta T_{M,S}$ ensured that we were well inside the chaotic regime described in [13–15], with a typical largest Lyapunov exponent of $\lambda \approx 3 \times 10^{-3}$ bits/s). The indices M and S refer to the master and slave system, respectively. These conditions produced amplitude oscillations with an "observed" [16] period of oscillation, $\tau_{M,S}$, of $\sim$166 s for the periodic case and $\sim$157 s for the chaotic flow. The coupling strength was determined by the variation of the flow rate of the cooling water: the smaller the flow rate, the larger the perturbation in the temperature of the circulating water produced by the master annulus. This allowed a maximum temperature perturbation of about $T_c^{RMS} = 0.02\,^\circ$C. For stronger coupling a computer-controlled auxiliary heater was later introduced to amplify the fluctuations output from the master. A temperature time variation in an AV regime for the unperturbed flow was digitally acquired, amplified, and fed back via the auxiliary heater to the cooling water that fed the outer (warm) circuit of the slave annulus. This auxiliary system allowed a coupling amplitude up to $T_c^{RMS} = 1.2\,^\circ$C. The dimensionless coupling strength was defined as $\eta = T_c^{RMS}/\Delta T_S$. A parametric mismatch between the systems was achieved by slightly altering the mean temperature contrast (ΔT_M) of the master system which, in turn, changed the natural AV oscillation period τ_M. This variation was almost linear (in the studied range) with a rate of about 1.8 s for every 0.1 °C. With the aid of the auxiliary heater, larger mismatches were also possible by digitally frequency shifting the acquired time series.

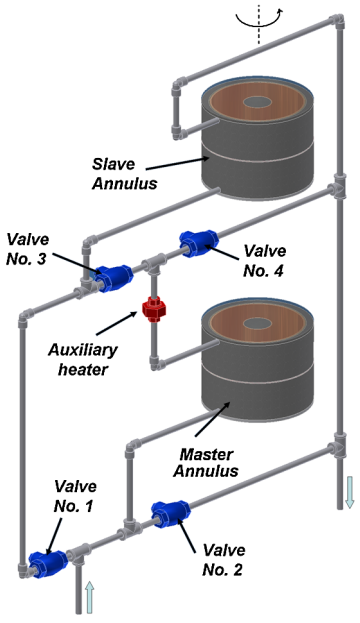

FIG. 1 (color online). A detailed diagram of the system coupled via the outer cooling water circuit highlighting the location of electric valves and the auxiliary heater. If valves No. 1 and No. 4 are closed, a coupled configuration is obtained.

Time series of the amplitude of the baroclinic waves (for each wave number) were obtained by applying Fourier transform techniques to the temperature measurement from the thermocouple ring for each system [13].

The detection of synchronization consisted mostly on the construction of the analytic signal and phase analysis, via the Hilbert transform (as described in [16,17]), for each system, $\Upsilon_M = X_M(t) + iX_M^H(t)$ and $\Upsilon_S = X_S(t) + iX_S^H(t)$, where $X_{M,S}(t)$ is the experimental time variation of the wave amplitude (around the temporal mean) and $X_{M,S}^H(t)$ its Hilbert transform. The phase is then obtained by computing: $\phi_{M,S}(t) = \arctan\frac{X_{M,S}^H(t)}{X_{M,S}(t)}$. The phase $\phi_{M,S}(t)$ is restricted by construction to the interval $[0, 2\pi]$. By accumulating the phases such that, following every cycle, $\phi_{M,S}$ increases by 2π, its increasing value in time can be observed. Finally, by calculating $\Delta\phi = \phi_M(t) - \phi_S(t)$, synchronization signatures can be investigated. Extra information to help in the identification of synchronized states was provided by histograms of $\Delta\phi(\text{mod}2\pi)$ and the value of the synchronization index $R = |\frac{1}{N}\sum_{k=1}^{N} e^{i\Delta\phi(t_k)}|$ [18] as a measure of phase coherence, yielding the value of unity only if the condition of full phase synchronization is fulfilled or zero for a uniform distribution of phases (expected for unsynchronized systems). The observed frequencies or periods [16] were also computed to study frequency entrainment.

Results.—Figure 2(i) shows time series of the phase difference $\Delta\phi$ between the natural AV modulation of each flow for four different values of mismatch with a constant coupling strength ($\eta = 2.1 \times 10^{-3}$). Figure 2(ii) presents the corresponding $\Delta\phi(\text{mod}2\pi)$ histograms. In this example, we can observe the transition from unsynchronized to synchronized states when the detuning is

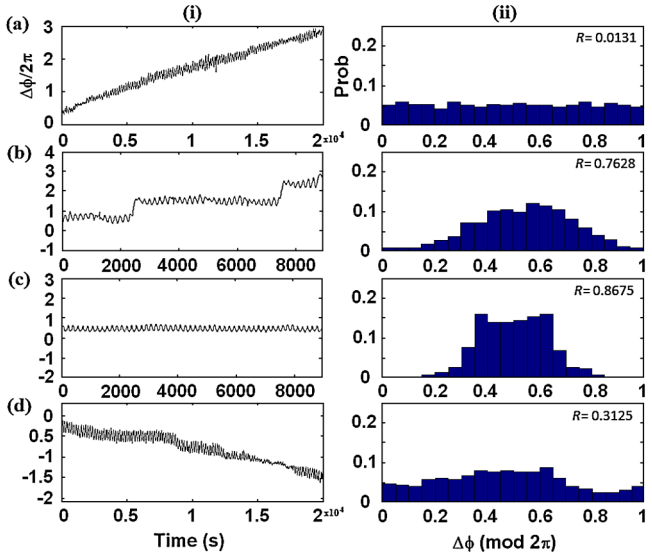

FIG. 2 (color online). (i) Time variation of the phase difference $\Delta\phi$ between the master system and the slave system, and (ii) histograms of $\Delta\phi$ (mod 2π), in the periodic AV regime, showing the transition from unsynchronized to partial and full phase synchronization for a constant coupling strength of $\eta = 2.1 \times 10^{-3}$ for (a) $\tau_M = 158.6$ s, (b) $\tau_M = 162.3$ s, (c) $\tau_M = 165.5$ s, (d) $\tau_M = 171.6$ s.

varied. Figures 2(b) and 2(c) show significant phase correlation. In particular, case 2(b) exhibits so-called phase slips, characteristic of coupled systems entering a synchronized Arnol'd tongue. Here the phase difference appears to remain constant for intervals but then jumps (2π jumps) rapidly to another value in an irregular series of small steps. As shown in Fig. 2(c), the systems reached full phase synchronization when the parameters of the two systems were sufficiently close (but not identical), as indicated by the approximate stationarity of $\Delta\phi$ and a clear peak in the $\Delta\phi(\mathrm{mod}2\pi)$ histogram. Figure 2(d) shows a continuously decreasing $\Delta\phi$, a signature of uncorrelated behavior, as we leave the synchronized region. A compilation of the experiments in the periodic AV case, plotted on a $\Delta\tau - \tau_M$ graph, where $\Delta\tau = \tau_S - \tau_M$, is presented Fig. 3. This figure clearly shows that the AV oscillation frequency of the slave system is being pulled towards that of the master system (so that $\Delta\tau \approx 0$) when the systems are actively interacting. The frequency entrainment region is clearly widened as the coupling strength is increased.

Even more remarkably, clear signatures of phase synchronization were also obtained in experiments in the chaotic AV regime. Figure 4 shows extracts of phase difference time series for varying mismatch of parameters. Larger coupling strengths (compared to the periodic case) were needed to reach full synchronization [Figs. 4(b) and 4(c)], presumably due to the higher complexity and amplitude variation in this chaotic regime. When added to the intrinsic and unavoidable natural experimental noise, this enhanced the apparition of phase slips, as shown in Fig. 4(a) and the desynchronization of

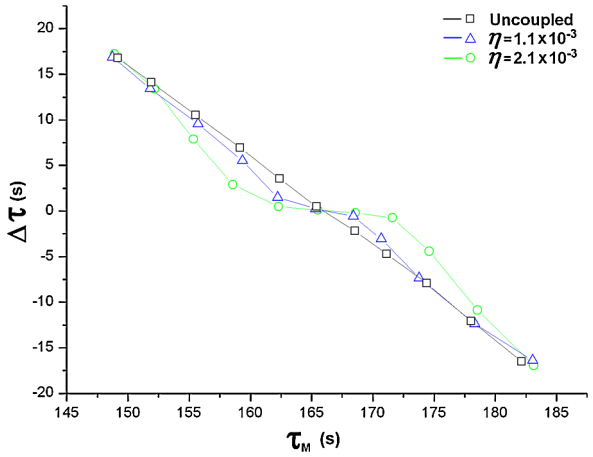

FIG. 3 (color online). Plots of oscillation period difference $\Delta\tau$ as function of η. A clear plateau is observed for small mismatches for the weakly coupled cases.

the systems, even when the two systems were very close in parameter space [as exemplified in Fig. 4(d)]. A collection of the experiments performed in this regime is presented in Fig. 5. As before, for relatively small detunings, the phase of the system is actively affected in such a way that its observed frequency becomes closer to that of the master, i.e., a signature of frequency entrainment. For larger couplings, clear phase synchronization for a large range of forcing periods was found. These results presented in Fig. 4 clearly demonstrate that the synchronized region increases in size as the coupling strength is increased.

Concluding remarks.—Synchronization between natural periodic, and more importantly, chaotic, oscillations was

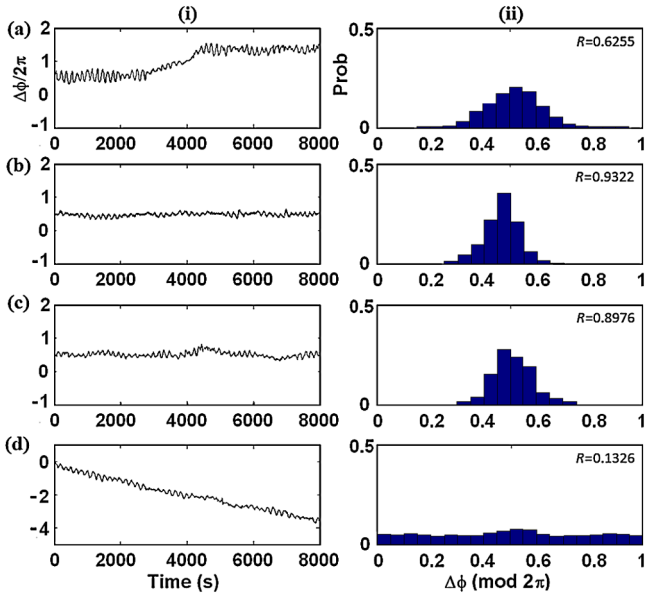

FIG. 4 (color online). As in Fig. 2 for the chaotic case. Demonstrating the transition to a synchronized state with constant $\eta = 1.25 \times 10^{-2}$ for (a) $\tau_M = 152$ s, (b) $\tau_M = 156.4$ s, (c) $\tau_M = 160.7$ s, (d) $\tau_M = 164.9$ s.

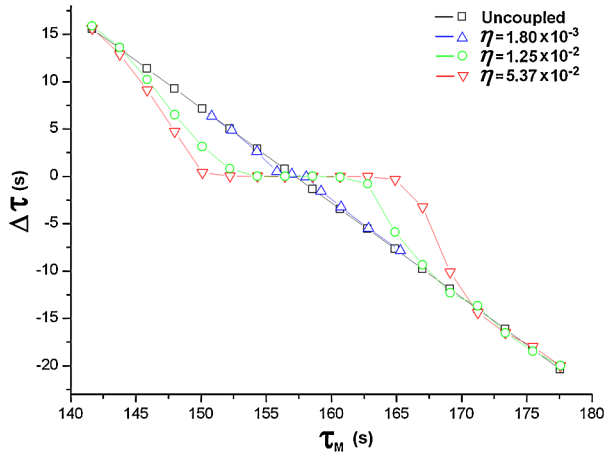

FIG. 5 (color online). As in Fig. 3 but for the chaotic case. Relatively large coupling strengths resulted in complete (phase) synchronization for a large range of mismatches.

found in our coupled experiment. We particularly emphasize the importance of having found synchronization in the chaotic regime since this is one of the first experiments to demonstrate synchronization of chaos in fluid dynamics. Furthermore, it provides a controlled laboratory analogue of teleconnected atmospheric phenomena (which are intrinsically chaotic in nature). For the periodic oscillation case, our results are similar to those found by [19], with the main difference that the signal now comes directly from another (nonidentical) system. Both sides of the mismatch range were explored, and synchronization was found reached even when the amplitude of the thermal perturbation (coupling) was extremely small. By coupling two annulus experiments via the thermal control of their outer (heated) sidewalls, we are effectively considering a schematic idealized interaction of two nearby, parallel, baroclinic zones, such as between the midlatitude or subtropical baroclinic zones in the northern and southern hemispheres of a planet. As discussed in [5], such an interaction might lead, for example, to near-simultaneous occurrence of blocking events in both hemispheres, and would constitute a form of indirect teleconnection. The nature and frequency of the occurrence of such teleconnected blocking events might be expected to depend on a number of factors, including the strength and coherence of interhemispheric coupling, and on season (which in turn affects the parametric relative ''detuning'' of the two hemispheres). These are situations that could, in the future, be modeled in our experimental setup. The case when $\Delta T_{M,S}$ in both annuli is the same could represents a planet with obliquity, $\varphi = 0$; i.e., the two hemispheres receive the same radiative heating. However, if $\Delta T_M \neq \Delta T_S$, we would be emulating a planet with a $\varphi \neq 0$. The method of coupling was introduced in our laboratory system is, of course, quite schematic when compared with explicit geophysical analogues. However, in light of this study it seems likely that synchronization effects are not particularly sensitive to the way in which the slave system is perturbed by the master.

It has been shown that some subtle entrainments and coherencies associated with higher order synchronization are invisible to correlation techniques (usually applied to the analysis of atmospheric data) and that, in general, phase analysis produces better quantitative results, in particular, in the estimation of the phase lag or difference between the two oscillatory phenomena [10,11]. It is therefore suspected that there are other cyclic phenomena which have only previously been investigated with these correlation techniques, in which some subtle but dynamically significant degrees of synchronization can be revealed if studied with modern time series tools based on phase analysis and phase synchronization approaches similar to those used in our experiment. The existence of such synchronization effects may have a strong influence on the behavior of weather systems and their potential predictability.

The authors acknowledge the U.K. Natural Environment Research Council for their support of this work.

[1] E. Tziperman, M. A. Cane, and S. E. Zebiak, J. Atmos. Sci. **52**, 293 (1995).
[2] J. M. Wallace, Q. J. R. Meteorol. Soc. **126**, 791 (2000).
[3] M. P. Baldwin *et al.*, Rev. Geophys. **39**, 179 (2001).
[4] J. Namias, J. Atmos. Sci. **7**, 130 (1950).
[5] G. S. Duane, P. J. Webster, and J. B. Weiss, J. Atmos. Sci. **56**, 4183 (1999).
[6] G. S. Duane, Phys. Rev. E **56**, 6475 (1997).
[7] G. S. Duane and J. J. Tribbia, Phys. Rev. Lett. **86**, 4298 (2001).
[8] F. Lunkeit, Chaos **11**, 47 (2001).
[9] Y. Feliks, M. Ghil, and A. W. Robertson (to be published).
[10] D. Maraun and J. Kurths, Geophys. Res. Lett. **32**, L15709 (2005).
[11] D. Rybski, S. Havlin, A. Bunde, Physica (Amsterdam) **320A**, 601 (2003).
[12] R. Hide and P. J. Mason, Adv. Phys. **24**, 47 (1975).
[13] P. L. Read, M. Collins, W.-G. Früh, S. R. Lewis, and A. F. Lovegrove, Chaos Solitons Fractals **9**, 231 (1998).
[14] P. L. Read, M. J. Bell, D. W. Johnson, and R. M. Small, J. Fluid Mech. **238**, 599 (1992).
[15] P. L. Read, Physica (Amsterdam) **58D**, 455 (1992).
[16] A. Pikovsky, M. Rosenblum, and J. Kurths, *Synchronization* (Cambridge University Press, Cambridge U.K., 2001).
[17] S. Boccaletti, J. Kurths, G. Osipov, D. L. Valladares, C. S. Zhou, Phys. Rep. **366**, 1 (2002).
[18] F. Mormann, K. Lehnertz, P. David, C. E. Elger, Physica (Amsterdam) **144D**, 358 (2000).
[19] F. J. R. Eccles, P. L. Read, A. A. Castrejon-Pita, and T. W. N. Haine, Phys. Rev. E **79**, 015202(R) (2009).